# Supporting Information

**Revealing the Role of Epithelial Mechanics and Macrophage Clearance during Pulmonary Epithelial Injury Recovery in the Presence of Carbon Nanotubes**

*Dedy Septiadi,* Wildan Abdussalam, Laura Rodriguez-Lorenzo, Miguel Spuch-Calvar, Joel Bourquin, Alke Petri-Fink, Barbara Rothen-Rutishauser**

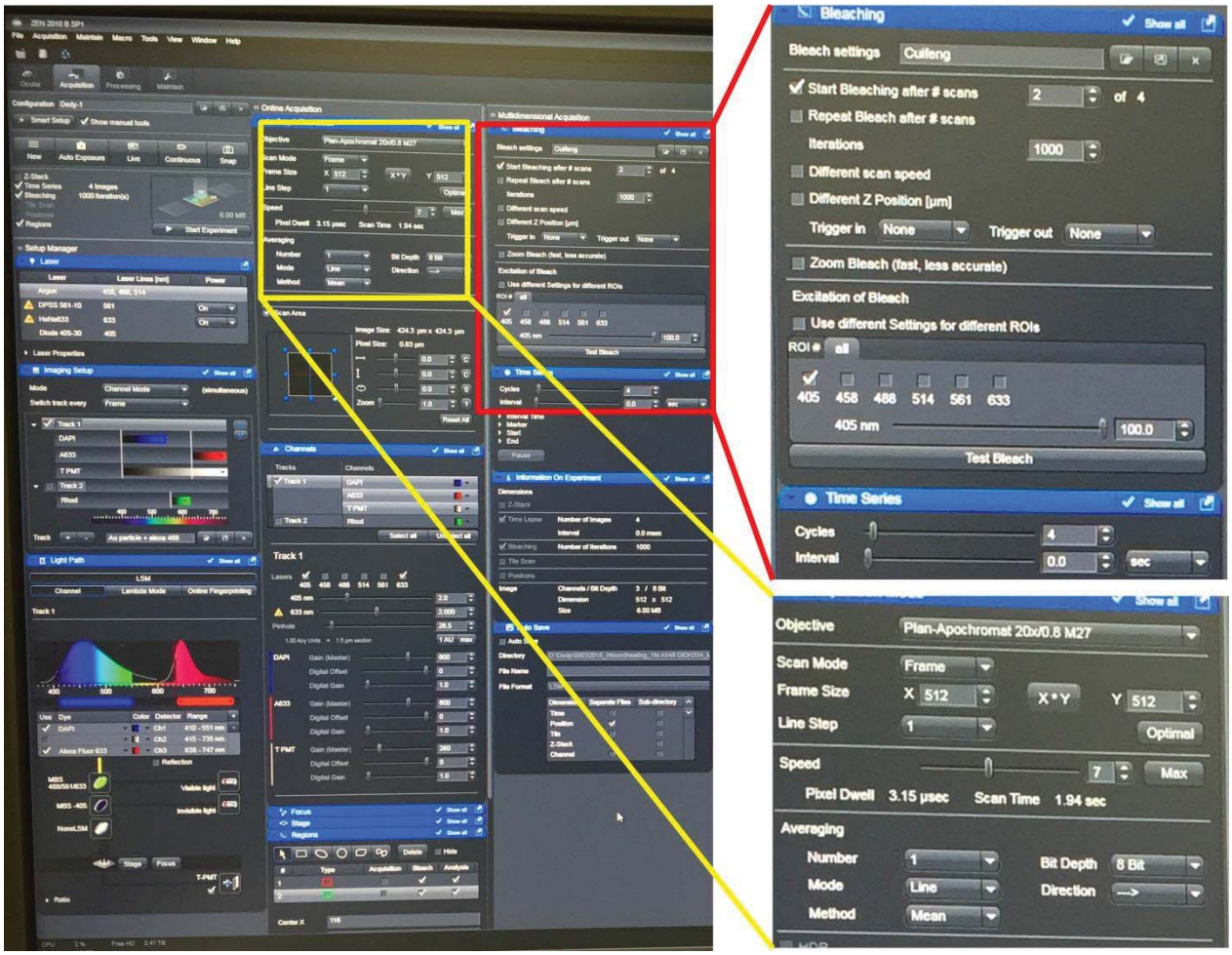


**Figure S1**. Extensive photobleaching module on LSM Zeiss 710 confocal microscope to simulate epithelial injury.

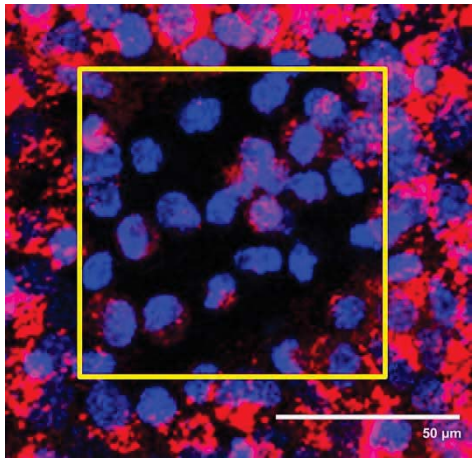


**Figure S2**. Confocal micrograph showing the number of dead cells inside the injury area (yellow square). Blue and red denotes nuclei and cytoplasm of epithelial cells, respectively. Cells were pre-stained with Hoechst 33342 and Vybrant® DiD cell-labeling solution, respectively.

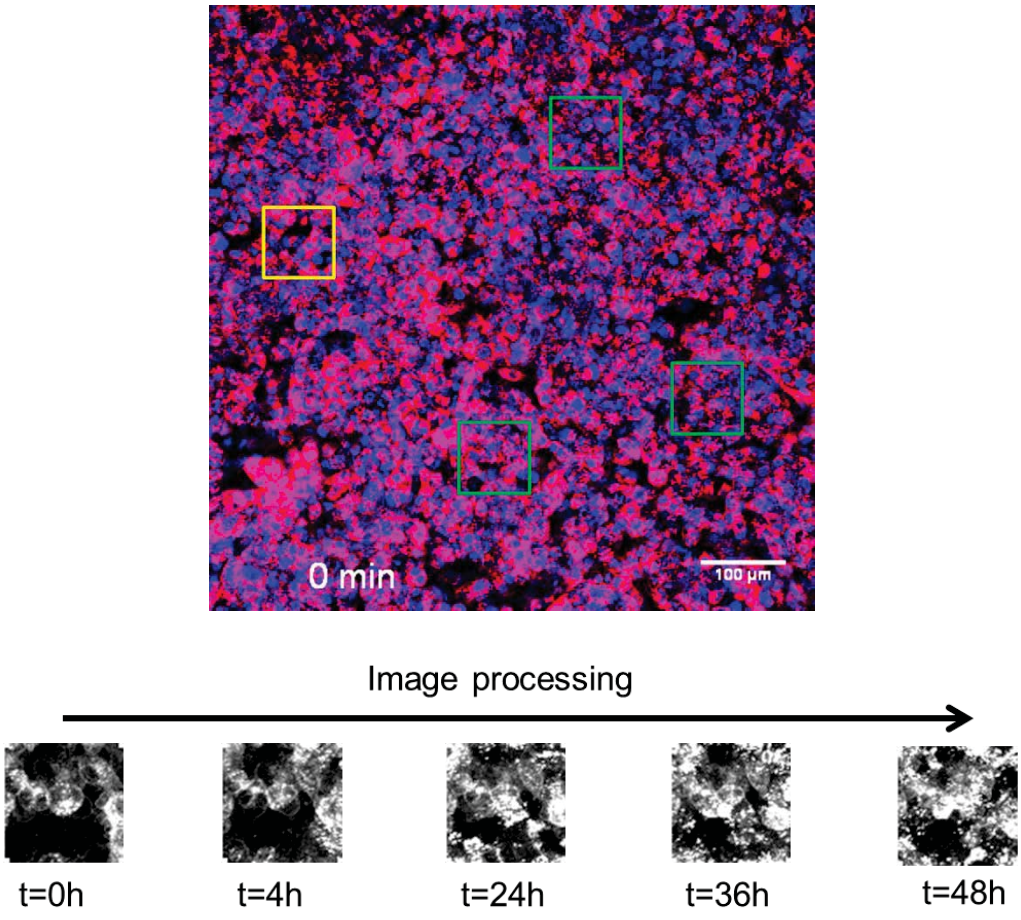


**Figure S3**. Quantification of the recovery rate by using image-processing. The invasion of live cells into the injury site (yellow square) over time was determined by measuring the pixel area

(i.e. surface area). Normalization of recovery rate was performed by comparing the obtained value with the average control value attained from non-bleached areas (green square).

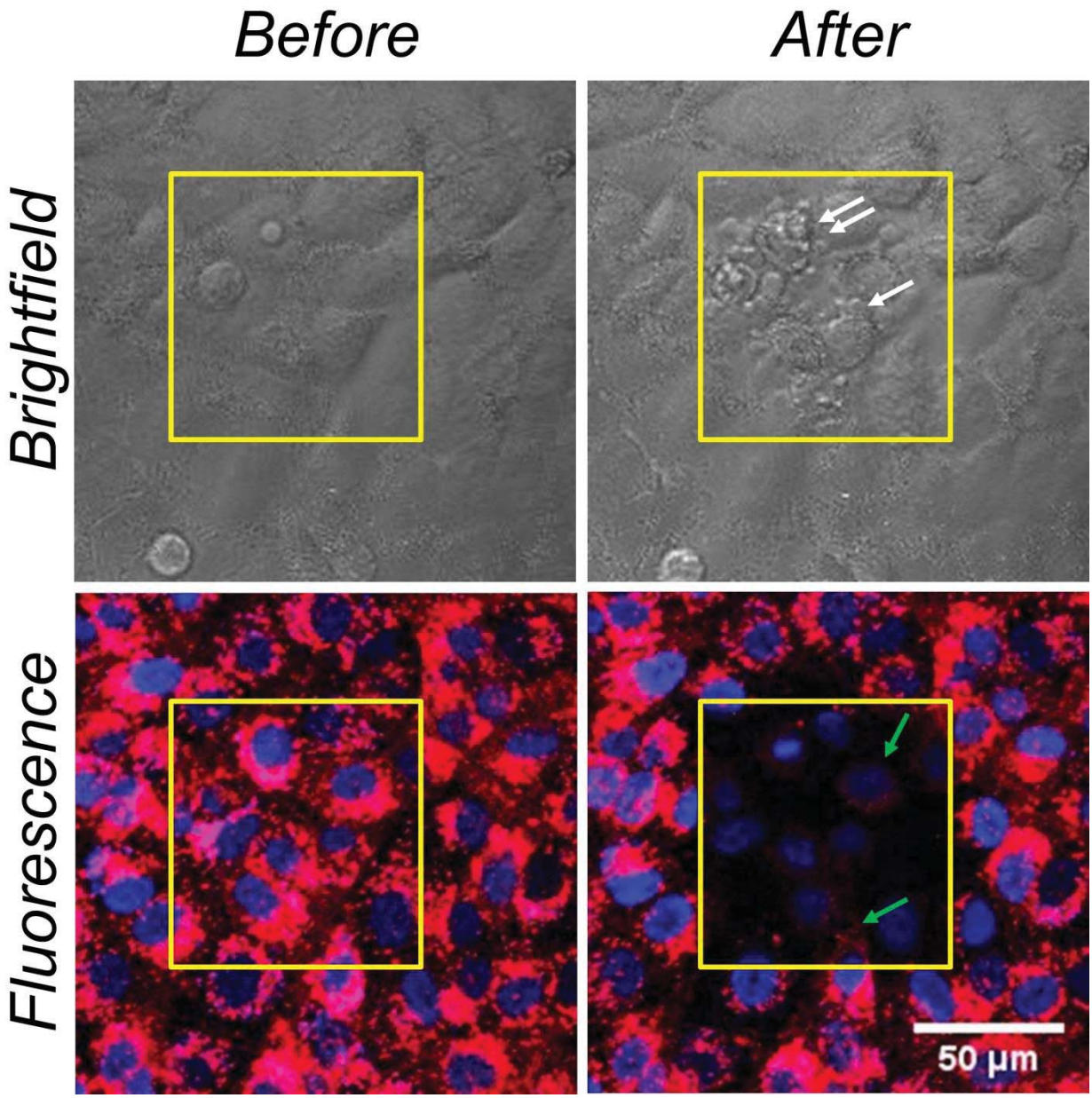


**Figure S4**. Comparison between the epithelial area before and after extensive photobleaching. Bright-field panels (top) show formation of apoptotic membrane blebbing (white arrows). Fluorescence channel (bottom) displays the presence of partially bleaching signal of the fluorescence dye. Red and blue corresponds to cytoplasm and nuclei, respectively whilst yellow square denotes the injury site.

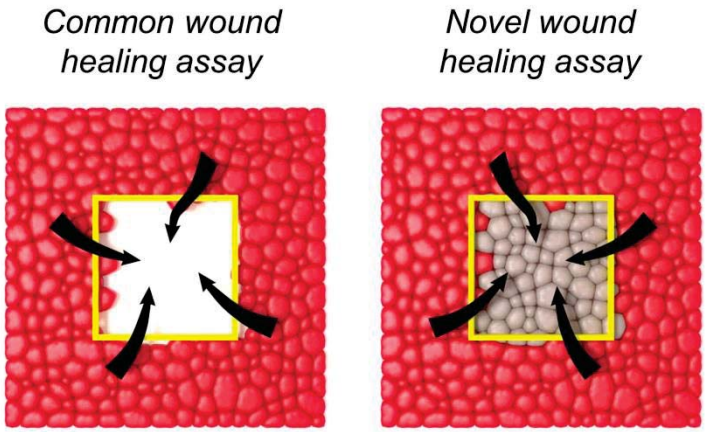


**Figure S5**. A schematic representation comparing most commonly used wound healing assay vs. novel developed assay. In our assay, no open area is available and dead cells (grey) are still intact, hence in order to lodge the space live cells (red) have to clear the dead cells first.

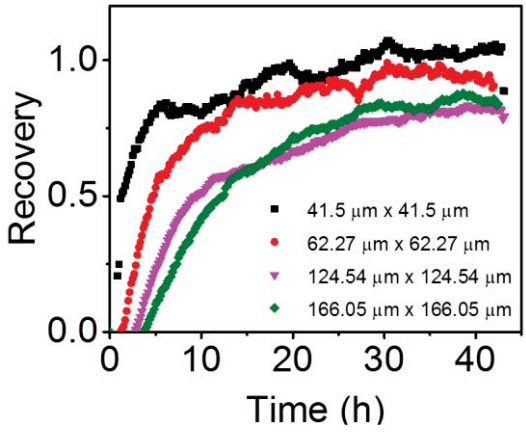


**Figure S6**. Recovery rate-injury size relationship. Data are shown as average value.

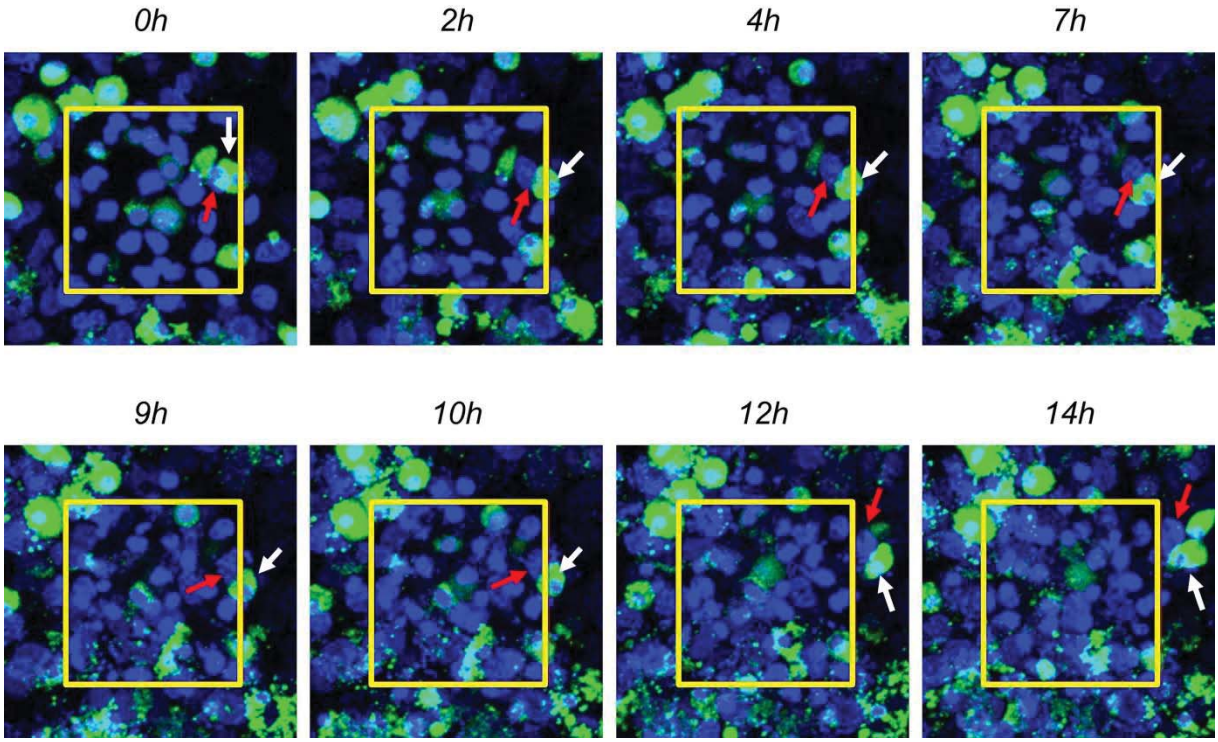


**Figure S7**. Time-lapse confocal micrographs showing ability of macrophages (green, white arrow) to pull dead epithelial cell (blue, red arrow) out of wound area (yellow square). Size of wound area is 83 µm × 83 µm.

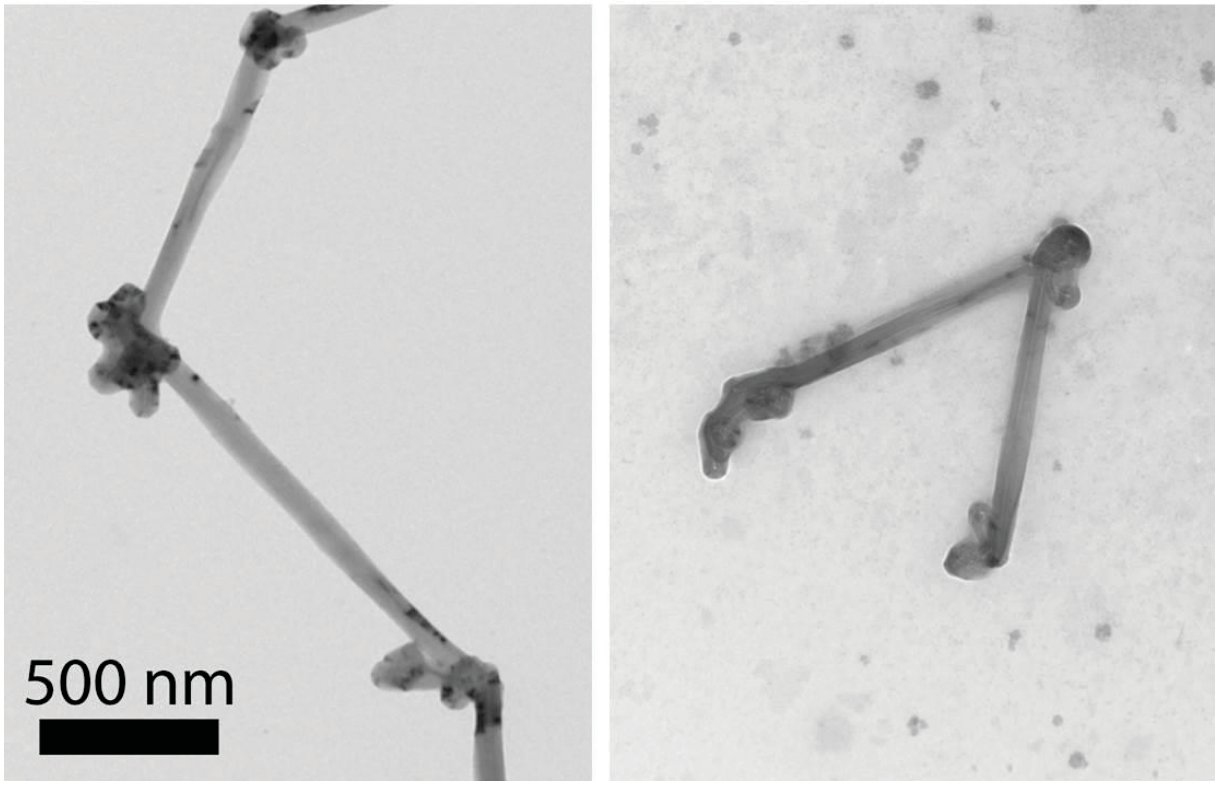


**Figure S8**. Representative transmission electron micrographs of Mitsui-7 CNTs dispersed in water (left) and in cell culture media (right).

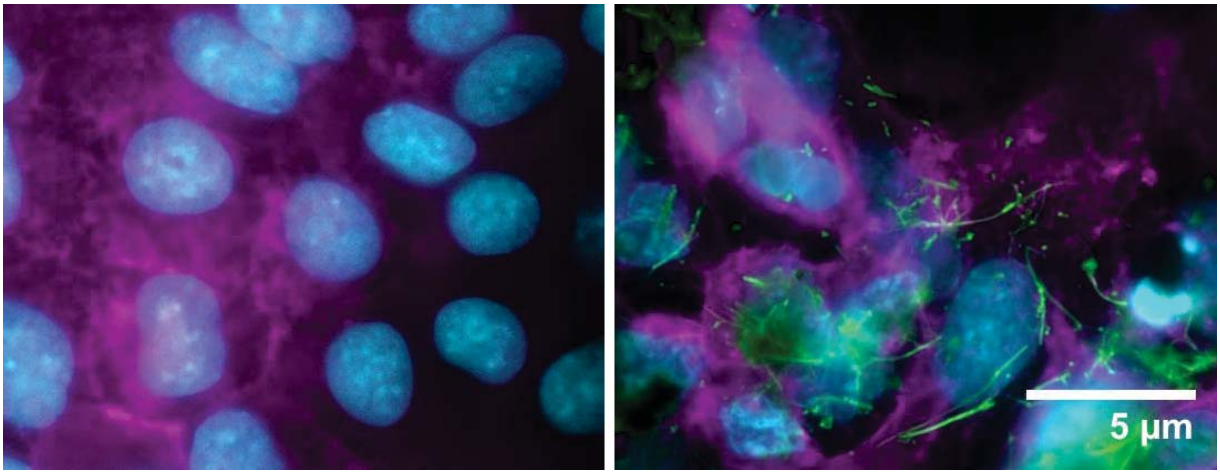


**Figure S9**. Enhanced darkfield and fluorescence micrographs of untreated cells (left) and cells treated with CNTs at administered dose 5 µg/mL (right). Cell nuclei, F-actin and CNTs are visible in cyan, magenta and green, respectively.

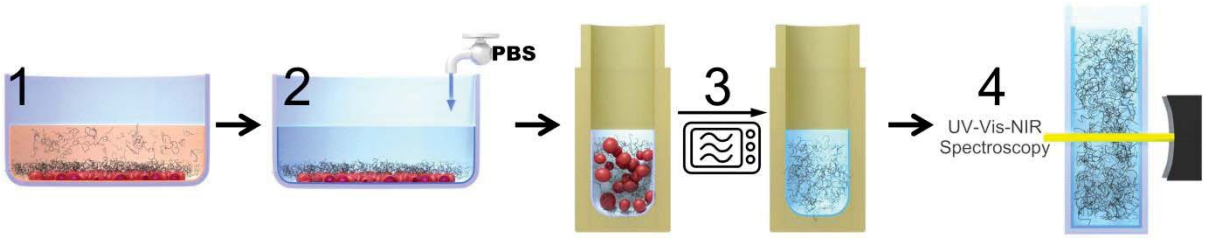


**Figure S10**. A scheme showing in vitro dosimetry of CNTs. The steps involve: (1) CNT exposure for 24h, (2) washing, (3) cell collection and microwave treatment, and (4) spectroscopy measurement.

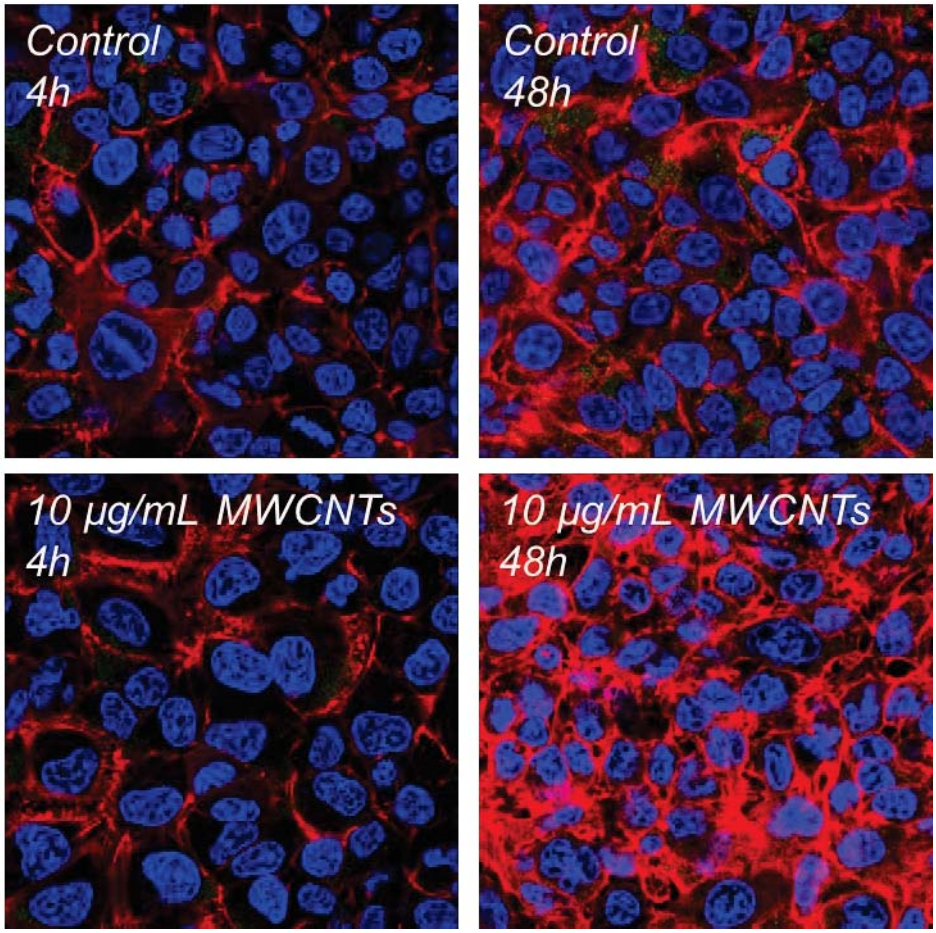


**Figure S11**. Confocal micrographs showing the formation of aberrant F-actins in A549 after incubation with CNTs. Cells possess thicker actin elements in comparison with non-treated cells (control). Blue represents nuclei and red is F-actin.

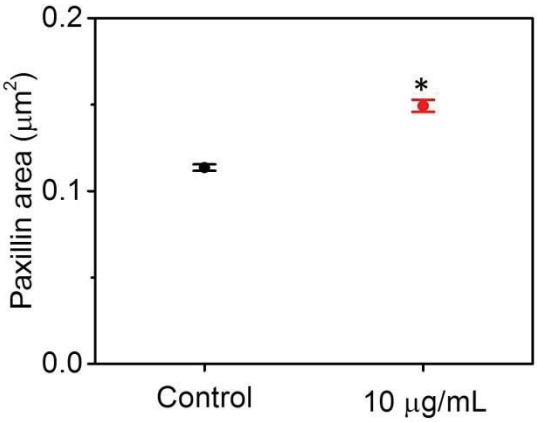


**Figure S12**. Quantification of size of paxillin focal adhesions by means of image processing. Data is shown as average area of paxillin and 95% confidence interval. One-way ANOVA, *$p$< 0.05. Number of analyzed paxillin for both cases is > 7,000.

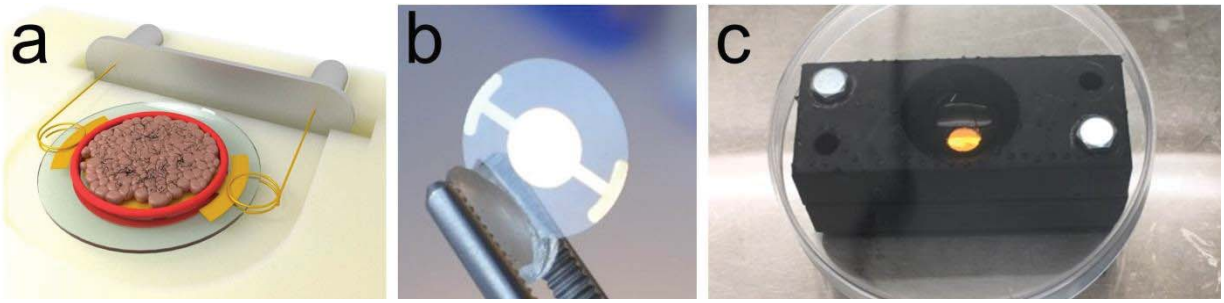


**Figure S13**. a) Schematic of quantification of cell adhesion using quartz crystal microbalance in in the presence of CNTs. Photograph of b) QCM gold substrate and c) Lab-made chamber allowing cultivation of the cells on the QCM substrate.

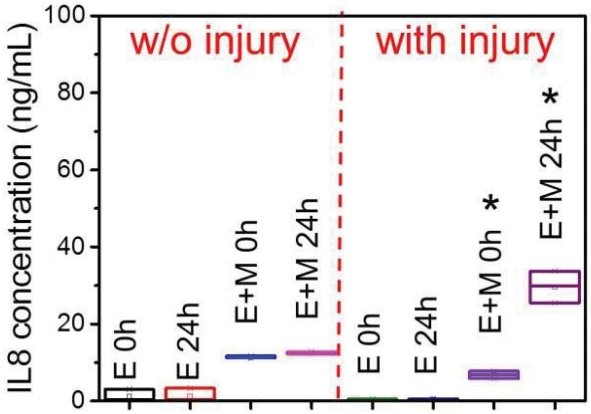


**Figure S14**. Production of IL8 chemokine in the presence and in the absence of injury at two different time points (i.e. 0h and 24h) in the co-culture systems measured by ELISA. Please note

that for all cases, 10 µg/mL CNTs was introduced on the systems. E and M denote epithelial and macrophages, respectively. One-way ANOVA, *$p$< 0.05.

**Section 1**. **Modeling of epithelial injury recovery**

We considered an ensemble of $N$ cells which were placed in neighboring sites of a two-dimensional lattice (**Figure S13a**). It consists of two constituents: (i) ”Living area”, the area occupied by the $N_l$ live cells, shown in blue; (ii) ”injury area”, the area occupied by the $N_d$ dead/apoptotic cells, shown in red. We assumed the cells possess a cylindrical symmetry shapes in which the shape fluctuations are restricted by the interdistance of the cell membrane and the center of the cell body $R$, to the width $\delta$ of fluctuating cell membrane [$R(\tau)$, $R(\tau) + \delta/2$] (**Figure S13b**) and they did not undergo mitosis.

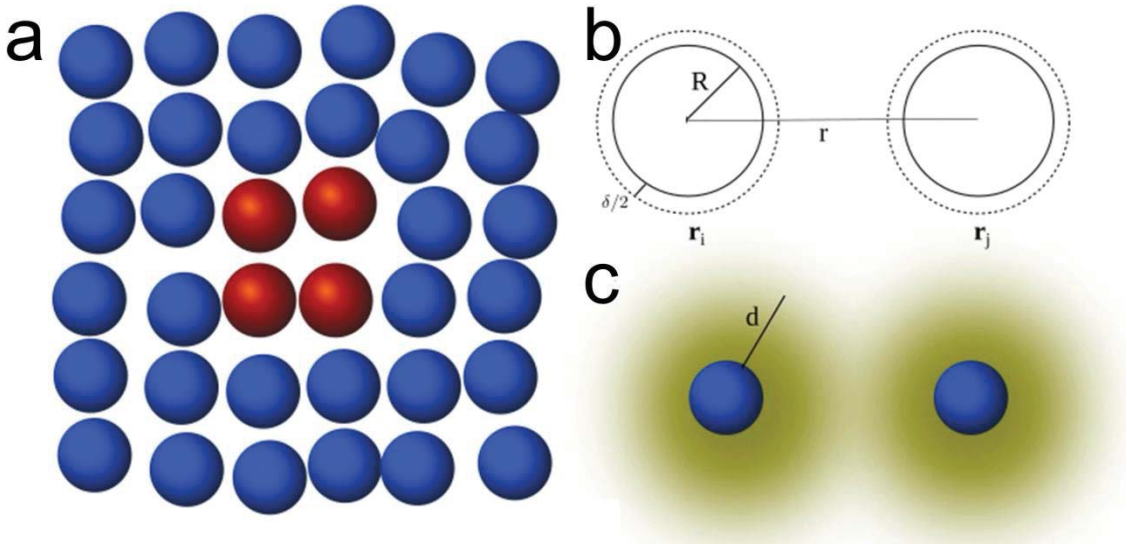


**Figure S13**. a) A schematic representation of the modeling of epithelial injury recovery. Blue and red circles indicate live and dead cells, respectively. At the initial configuration of the simulation, all cells are at rest. b) Interdistance cells are taken from their center of mass in which each cell possesses a radius $R + \delta/2$ and c) interaction range $d$.

The state $S_i$ of a cell $i$ is described by its position, which is given by the vector $r_i$of its center of mass. A pair of cells at a vector $r_i$ and $r_j$ experiences a short-range interaction $V_{ij} = V_o/|r_i - r_j|$ with an interaction strength $V_o > 0$ and $|r_i - r_j| > R$. The force experienced by the inner cell $i$ due to its neighbors $j$ reads:

$$F(S_i) = \sum_{i<j} V_{ij} n_j \qquad (Equation\ 1)$$

Where $n_j$ denotes the number of neighboring-living cell $i$. The dead cells are at rest and the cell dynamics follows a two-dimensional random walk,[1-3] in which their probabilities are determined by the Metropolis algorithm.[4] Specifically, individual migration of cell $i$ occurs with the acceptance probability $\exp(-[F(\bar{S}_i) - F(S_i)])$, where $\bar{S}_i$ and $S_i$ are a state after and before the accepted movement, respectively. The individual migration trial consists of a shift $r_i \rightarrow r_i + \Delta r_i$ of cell $i$ in a random direction within interval $\Delta r_i = [0, \eta]$.

Due to the presence of stress forces, the outermost cells push their inner neighbors such that the living cells move towards the wound area and apply a pressure (epithelial pushing) on the outer dead cells. Consequently, the dead cells are pushed out of substrate provided that $|r_i - r_j| < r_{min}$ in which $r_{min} < R$. As dead cells left the substrate, their positions are gradually replaced by the living cells (**Video S2**). We subsequently compared the migration rate of an aforementioned case to the ensemble of cells in the presence of carbon nanotubes which serves as dissipation. As a result, it gives rise to the force dissipation of each cell $F_i$which reads:

$$F_i = \gamma + \sum_{i<j} V_{ij} n_j \qquad (Equation\ 2)$$

where $\gamma$ denotes force dissipation due the presence of carbon nanotubes. Following our experimental setup, we obtained a density of cells in an ensemble where, $\rho \simeq 5.81 \times 10^5\ cells/cm^2$. Consequently, the total number of simulated cells $N_{cells} \approx 1{,}049 \simeq 32 \times 32$ which contains $N_d \approx 6 \times 6$ and $N_l \approx 1{,}013$ cells in the wound and active areas, respectively. We considered the average radius of the cells $R = 10 \pm 0.01\ \mu m$, the pair of cells experiences the interaction strength $V_o \approx 1.0\ \mu Hz$, with $\eta = 1\ \mu m$ and $d \approx 80\ \mu m$. To further understand effects of CNTs on the migration processes, we compared the movement rates of living cells in the

absence and the presence of the CNTs. To qualitatively mimic the latter case in which CNTs with concentration 5 and 10 μg/mL were present, we proposed two different parameters of $\gamma = 0.5\ \mu Hz$ and $\gamma = 1.0\ \mu Hz$. For $\gamma = 0.5\ \mu Hz$, we observed a slowdown of migration of living cells compared to the case where dissipation is absent (untreated cell, **Video S6**). Moreover, as dissipation increased to $\gamma = 1.0\ \mu Hz$ (i.e. corresponds to higher concentration of CNTs), the migration rate decreased further (**Video S7**). This can be understood as follows. As the forces exerted and experienced by CNT-treated epithelial cells increase (**Video S8-S9**), their acceptance probability in moving to a new site decreases. As a result, this slows down the migration process and prevents quick wound recovery. This finding is in qualitative agreement with our experimental results (see **Figure 3a** from the main text).

**Supporting Video**

**Video S1**. Time-lapse fluorescence (left) and bright-field (right) video showing the recovery of epithelial injury. Individual cell migration and epithelial mechanics (epithelial pushing force) is responsible for clearance of dead cells and further, lodging the injury site. Blue and red show the cell nuclei and cytoplasm of epithelial cells, respectively. The red square denotes the injury area.
**Video S2.** Computer simulation revealing the role of epithelial mechanics (pushing) in the recovery of epithelial injury. Live epithelial cells (blue) push apoptotic cells (red) allowing detachment of dead cells from the substrate and subsequently filling in the space.
**Video S3.** Computed force exerted by live epithelial cells to their neighbors. Dead cells in the middle were at rest, hence force ≈ 0 MHz.
**Video S4.** Time-lapse video showing the involvement of macrophages (MDMs, green) in the clearance of apoptotic epithelial cells. In blue and red are the cell nuclei and cytoplasm of epithelial cells, respectively. The red square denotes the injury area.
**Video S5.** Time-lapse video displaying different kinetics of injury recovery in the absence (left) and in the presence of CNTs at initial concentration 10 μg/mL. Slower recovery was recorded in the CNT-treated epithelial cells. Blue and red represent the cell nuclei and cytoplasm of epithelial cells, respectively. Center of the window denotes the injury area.
**Video S6**. Computer simulation showing the retardation of the recovery of epithelial injury in the presence of CNTs at initial concentration 5 μg/mL. CNTs serve as dissipation or disturbance, hence slowing individual epithelial migration.
**Video S7**. Computer simulation showing the retardation of the recovery of epithelial injury in the presence of CNTs at initial concentration 10 μg/mL. CNTs serve as dissipation or disturbance, hence slowing individual epithelial migration.

**Video S8**. Computed force (in $\mu Hz$) exerted by CNT-treated epithelial cells to their neighbors. Cells possessed higher force in comparison to the untreated one (see **Video S3**). CNTs' initial concentration 5 μg/mL.
**Video S9**. Computed force (in $\mu Hz$) exerted by CNT-treated epithelial cells to their neighbors. Cells possessed higher force in comparison to the untreated one (see **Video S3**). CNTs' initial concentration 10 μg/mL.
**Video S10**. Time-lapse bright-field (left) and fluorescence (right) video showing the internalization of CNTs (dark) by macrophages (MDMs, green) on epithelial carpets (red). CNTs' initial concentration 10 μg/mL.
**Video S11**. Time-lapse bright-field/fluorescence (left) and fluorescence (right) video showing the internalization of CNTs (dark) by macrophages (MDMs, green) on epithelial carpets (red and blue) following by restoration of injury recovery. CNTs' initial concentration 10 μg/mL. Blue and red represent the cell nuclei and cytoplasm of epithelial cells, respectively. Center of the window denotes the injury area.

Reference


1 Codling, E. A., Plank, M. J. & Benhamou, S. *J R Soc Interface* **5**, 813-834, (2008).
2 Bressloff, P. C. *Stochastic Processes in Cell Biology*. (Springer, 2014).
3 Berg, H. C. *Random Walks in Biology*. (Princeton University Press, 1993).
4 Metropolis, N., Rosenbluth, A. W., Rosenbluth, M. N., Teller, A. H. & Teller, E. *The Journal of Chemical Physics* **21**, 1087-1092, (1953).